

Caudrelier, V., Mintchev, M. & Ragoucy, E. (2013). Quantum wire network with magnetic flux. *Physics Letters A*, 337(31-33), pp. 1788-1793. doi: 10.1016/j.physleta.2013.05.018



**CITY UNIVERSITY  
LONDON**

[City Research Online](#)

**Original citation:** Caudrelier, V., Mintchev, M. & Ragoucy, E. (2013). Quantum wire network with magnetic flux. *Physics Letters A*, 337(31-33), pp. 1788-1793. doi: 10.1016/j.physleta.2013.05.018

**Permanent City Research Online URL:** <http://openaccess.city.ac.uk/2442/>

#### **Copyright & reuse**

City University London has developed City Research Online so that its users may access the research outputs of City University London's staff. Copyright © and Moral Rights for this paper are retained by the individual author(s) and/ or other copyright holders. All material in City Research Online is checked for eligibility for copyright before being made available in the live archive. URLs from City Research Online may be freely distributed and linked to from other web pages.

#### **Versions of research**

The version in City Research Online may differ from the final published version. Users are advised to check the Permanent City Research Online URL above for the status of the paper.

#### **Enquiries**

If you have any enquiries about any aspect of City Research Online, or if you wish to make contact with the author(s) of this paper, please email the team at [publications@city.ac.uk](mailto:publications@city.ac.uk).

# Quantum Wire Network with Magnetic Flux

Vincent Caudrelier<sup>1</sup>, Mihail Mintchev<sup>2</sup> and Eric Ragoucy<sup>3</sup>

<sup>1</sup> *Center for Mathematical Science, City University London, Northampton Square, London EC1V 0HB, UK*

<sup>2</sup> *Istituto Nazionale di Fisica Nucleare and Dipartimento di Fisica dell'Università di Pisa, Largo Pontecorvo 3, 56127 Pisa, Italy*

<sup>3</sup> *LAPTh, Laboratoire d'Annecy-le-Vieux de Physique Théorique, CNRS, Université de Savoie, BP 110, 74941 Annecy-le-Vieux Cedex, France*

(Dated: May 14, 2013)

The charge transport and the noise of a quantum wire network, made of three semi-infinite external leads attached to a ring crossed by a magnetic flux, are investigated. The system is driven away from equilibrium by connecting the external leads to heat reservoirs with different temperatures and/or chemical potentials. The properties of the exact scattering matrix of this configuration as a function of the momentum, the magnetic flux and the transmission along the ring are explored. We derive the conductance and the noise, describing in detail the role of the magnetic flux. In the case of weak coupling between the ring and the reservoirs, a resonant tunneling effect is observed. We also discover that a non-zero magnetic flux has a strong impact on the usual Johnson-Nyquist law for the pure thermal noise at small temperatures.

Corresponding author: v.caudrelier@city.ac.uk, tel: +44(0)2070408498.

## I. INTRODUCTION

In this paper we investigate the effect of ambient electromagnetic fields on quantum wire networks. We focus on the network displayed in left hand side of fig. 1, composed of a ring enclosing a magnetic flux  $\phi$ , and three semi-infinite leads. The *one-body* interactions at the vertices  $V_j$  are described by local scattering matrices  $S_j$ , whereas along both the internal and external edges  $E_i$  the charges interact with a time-independent ambient electromagnetic field, generated by a classical potential  $\mathbf{A}(\mathbf{x})$ . We show that all these interactions can be incorporated in a *fully equivalent* total scattering matrix  $S^\phi$ , leading to the effective Y-junction in the right hand side of fig. 1. It is worth mentioning that the *critical* (scale invariant) conductance properties of Y-junctions and their phase diagram have been previously investigated by different methods like bosonization<sup>1-9</sup>, renormalization group and scattering techniques<sup>10-16</sup> and conformal field theory<sup>17,18</sup>. We concentrate below on some *off-critical* aspects, establishing first the exact form of  $S^\phi$ . We discuss afterwards both the conductance and the noise at finite temperature and discover some new features, related to the finite size of the ring and the non-trivial magnetic flux.

The system is driven away from equilibrium by attaching to the external leads thermal reservoirs at (inverse) temperatures  $\beta_i$  and chemical potentials  $\mu_i$ , as shown in fig. 2. Our main goal is to study the transport properties and the noise of this configuration as a function of the transmission  $\mathbf{t}$  in the ring, the flux  $\phi$ , the temperatures  $\beta_i$  and the chemical potentials  $\mu_i$ . We show that Aharonov-Bohm type oscillations with  $\phi$  occur in both the conductance and the noise. The period of these oscillations equals the elementary flux quantum  $\phi_0 = 2\pi\hbar c/e$  associated with a single charge  $e$ . We find that the pure thermal noise has a  $\phi$ -dependent power law behavior at small temperatures which interpolates between the usual

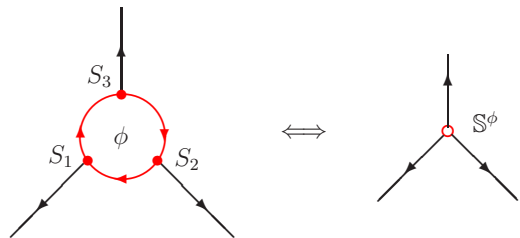


FIG. 1: (Color online) Ring junction with local  $S$ -matrices  $\{S_j : j = 1, 2, 3\}$  and magnetic flux  $\phi$  (left) and its Y-junction counterpart with equivalent total scattering matrix  $S^\phi$  (right).

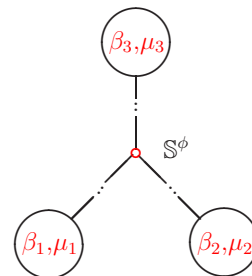


FIG. 2: (Color online) Y-junction connected at infinity to thermal reservoirs with temperature  $\beta_i$  and chemical potential  $\mu_i$ .

linear Johnson-Nyquist behavior and a new, quadratic behavior for values of  $\phi$  greater than a critical value  $\phi_c$  which we quantify. Finally, as functions of  $\mu_i$ , the current and the shot noise show in the regime  $\mathbf{t} \sim 1$  an interesting plateaux structure, which is related to a resonant tunneling effect. The fundamental and essentially unique input for deriving these results is the requirement of self-adjointness of the Schrödinger Hamiltonian with magnetic flux  $\phi$  on the graph in fig. 1.

We would like to mention also that the wires, displayed in the figures of this paper, are planar and in most of the cases have straight line edges. However, the discussion below is completely general and applies to segments of arbitrary smooth curves in  $\mathbb{R}^3$  as well. What is essential is to have a well defined tangent vector field along the edges  $E_i$ ,  $i = 1, 2, 3$ , in order to define the projection  $A_x(x, i)$  of the ambient field  $\mathbf{A}(\mathbf{x})$  on the graph.

## II. BULK DYNAMICS AND LOCAL VERTEX INTERACTIONS

The dynamics in each edge is defined by the Schrödinger equation (we use natural units  $c = \hbar = 1$ )

$$\left[ i\partial_t + \frac{1}{2m} (\partial_x - ieA_x(x, i))^2 \right] \psi(t, x, i) = 0, \quad (1)$$

where  $(x, i)$  are local coordinates on  $E_i$ . Besides the bulk dynamics, we have to introduce also the interaction at the vertices  $V_j$ , which represents a subtle point. Some recent developments<sup>19,21</sup> in the spectral theory of operators on graphs have shown that these two ingredients are not independent<sup>22,23</sup>, *if one requires unitary time-evolution of the system*. The reason is that the time evolution in the bulk is described by a *Hermitian* Hamiltonian, which becomes *self-adjoint* only by imposing special boundary conditions at the vertices. These conditions generate *particular* point-like interactions, which are described by specific (and not arbitrary) scattering matrices  $S_j$ , associated with each vertex  $V_j$  of the graph. Let us illustrate the phenomenon using for simplicity the bulk Hamiltonian  $-\partial_x^2$  corresponding to (1) with  $e = 0$ . Assume that the vertex  $V$  with local coordinate  $x = 0$  is the origin of  $n$  edges  $E_i$ . The most general boundary condition ensuring that  $-\partial_x^2$  has a self-adjoint extension at  $x = 0$  is<sup>19-21</sup>

$$\sum_{j=1}^n [\lambda(\mathbb{I} - U)_{ij} \psi(t, 0, j) - i(\mathbb{I} + U)_{ij} (\partial_x \psi)(t, 0, j)] = 0, \quad (2)$$

where  $U$  is an arbitrary  $n \times n$  unitary matrix and  $\lambda$  is a real parameter with the dimension of mass.  $U = \mathbb{I}$  and  $U = -\mathbb{I}$  generalize to a vertex with multiple edges the familiar Neumann and Dirichlet boundary conditions on the half line. The point-like interaction, induced by (2), generates<sup>19,21</sup>

$$S(k) = -\frac{[\lambda(\mathbb{I} - U) - k(\mathbb{I} + U)]}{[\lambda(\mathbb{I} - U) + k(\mathbb{I} + U)]}, \quad k \in \mathbb{R}, \quad (3)$$

which defines a family of unitary scattering matrices parametrized by  $U \in U(n)$ , with a special momentum dependence.  $S(k)$  is a meromorphic function with simple poles, all of which located on the imaginary axis and different from 0. It turns out<sup>8</sup> that  $S(k)$  preserves time reversal invariance if and only if  $S(k)$  is *symmetric*. We will use this information when discussing below the breaking of time reversal symmetry caused by the magnetic flux.

The critical (scale-invariant, i.e.  $k$ -independent) points  $S^c = S(k = \lambda) = U$  in the family (3) capture the universal features of the local vertex interactions and play therefore a distinguished role. Furthermore, imposing time-reversal invariance implies<sup>8</sup> that  $S^c$  is a symmetric matrix belonging to the orthogonal group  $O(n)$ . Let us consider the case  $n = 3$ , relevant for the Y-junction in fig. 1, and let us assume that the internal edges of each local junction are equivalent as far as transmission and reflection are concerned. Labeling these edges by the indices 2 and 3, the matrix elements of  $S^c$  must be invariant under the exchange  $2 \leftrightarrow 3$ . These requirements fully determine the solutions for  $S^c$  which are of two types. There are two one-parameter families

$$S_{\pm}^c(\mathbf{t}) = \pm \begin{pmatrix} 1 - 2\mathbf{t} & \epsilon\sqrt{2\mathbf{t}(1-\mathbf{t})} & \epsilon\sqrt{2\mathbf{t}(1-\mathbf{t})} \\ \epsilon\sqrt{2\mathbf{t}(1-\mathbf{t})} & \mathbf{t} - 1 & \mathbf{t} \\ \epsilon\sqrt{2\mathbf{t}(1-\mathbf{t})} & \mathbf{t} & \mathbf{t} - 1 \end{pmatrix}, \quad (4)$$

where  $\epsilon^2 = 1$  and  $\mathbf{t} \in (0, 1)$  is the *transmission coefficient* controlling the local tunneling between the edges 2 and 3 of the junction. And there are eight discrete solutions which we discard in the following as they describe disconnected external leads. Since  $\det(S_{\pm}^c) = \pm 1$ , the matrices (4) belong to the two disconnected components of  $O(3)$ . The matrix  $S_{\pm}^c(\mathbf{t} = 1/2)$  (with  $\epsilon = 1$ ) has been introduced in Ref.<sup>33</sup>. In<sup>34</sup> the matrices  $S_{\pm}^c(\mathbf{t})$  (with  $\epsilon = 1$ ) have been considered for generic  $\mathbf{t} \in [0, 1]$ . We argued above that  $S_{\pm}^c(\mathbf{t})$  are critical points in the set of all scattering matrices ensuring the self-adjointness of the Schrödinger Hamiltonian on the graph in fig. 1.

The above considerations can be extended to the case  $e \neq 0$ , performing the shift  $\partial_x \mapsto \partial_x - ieA_x(x, i)$  in eq. (2). Introducing the magnetic flux

$$\phi = \oint_C \mathbf{A}(\mathbf{x}) \cdot d\mathbf{l}, \quad (5)$$

where  $C$  is the ring in fig. 1, the shift generates  $e\phi$ -dependent phases that charges pick up traveling along the edges. These phases are transferred<sup>29,35</sup> by a kind of “gauge” transformation to the matrix  $U$  and therefore to  $S(k)$ . We set for simplicity  $e = 1$  in the rest of the paper.

## III. THE TOTAL SCATTERING MATRIX $\mathbb{S}^{\phi}$

The problem now is to reconstruct the total scattering matrix  $\mathbb{S}^{\phi}$  in fig. 1 from the local ones. Several equivalent schemes<sup>24-28</sup> exist for facing this problem. We follow below the approach of<sup>28</sup>, which adapts better to the case with ambient magnetic field and provides explicit expressions. Since the form of  $\mathbb{S}^{\phi}$  for a generic ring junction with general local scattering matrices is quite complicated, we simplify the considerations by focusing on the case of *identical* local scattering matrices given by (4) and *equidistant* vertices, separated by a distance  $d$  along the ring. In this case the system is invariant under cyclic

permutations, implying that  $\mathbb{S}^\phi$  is a *circulant* matrix, i.e.

$$\mathbb{S}_\pm^\phi(k) = \begin{pmatrix} \sigma_1^\pm(k, \phi) & \sigma_2^\pm(k, \phi) & \sigma_3^\pm(k, \phi) \\ \sigma_3^\pm(k, \phi) & \sigma_1^\pm(k, \phi) & \sigma_2^\pm(k, \phi) \\ \sigma_2^\pm(k, \phi) & \sigma_3^\pm(k, \phi) & \sigma_1^\pm(k, \phi) \end{pmatrix}, \quad (6)$$

where<sup>35</sup>

$$\sigma_j^\pm(k) = \frac{1}{3} \sum_{\ell=1}^3 e^{i\frac{2\pi}{3}(1-\ell)(j-1)} \lambda_\pm \left( k, \frac{\phi + 2(\ell-1)\pi}{3} \right), \quad (7)$$

with

$$\lambda_\pm(k, \theta) = \mp \frac{\mathbf{t}(\cos \theta \mp \cos kd) \pm i(\mathbf{t} - 1) \sin kd}{\mathbf{t}(\cos \theta \mp \cos kd) \mp i(\mathbf{t} - 1) \sin kd}. \quad (8)$$

Although the local scattering matrices are  $k$ -independent and  $\epsilon$ -dependent, the total one depends on the parameter  $kd$ , involving the size of the ring, but not on  $\epsilon$ .

Equations (6, 7, 8) represent a fundamental point of our investigation and determine the following set of total scattering matrices  $\{\mathbb{S}_\pm^\phi(k; d, \mathbf{t}) : d \geq 0, \mathbf{t} \in [0, 1]\}$ . Since

$$\mathbb{S}_\pm^\phi(k; 0, \mathbf{t}) = \mp \mathbb{I}, \quad (9)$$

which describe three *disconnected* edges, we take in the rest  $d \neq 0$ . Moreover, since

$$\mathbb{S}_-^\phi(k; d, \mathbf{t}) = -\mathbb{S}_+^{(\phi+\pi)}(k; d, \mathbf{t}), \quad (10)$$

without loss of generality we concentrate in what follows on  $\mathbb{S}_+^\phi$ , omitting for simplicity the index  $+$ . Observing that

$$\sigma_2(k, \phi) \neq \sigma_3(k, \phi), \quad \text{for } \phi \neq 3n\pi, \quad n \in \mathbb{Z}, \quad (11)$$

we conclude that time reversal invariance is broken ( $\mathbb{S}^\phi$  is not symmetric), except for the fluxes  $\phi = 3n\pi$ .

We focus at this point on the *transmission amplitudes*

$$\tau_+(k, \phi) \equiv |\sigma_2(k, \phi)|, \quad \tau_-(k, \phi) = |\sigma_3(k, \phi)|, \quad (12)$$

and the *reflection amplitude*

$$\varrho(k, \phi) \equiv |\sigma_1(k, \phi)|, \quad (13)$$

which satisfy (due to unitarity) the expected relation

$$\varrho^2(k, \phi) + \tau_+^2(k, \phi) + \tau_-^2(k, \phi) = 1, \quad (14)$$

among probabilities. One can verify that both  $\tau_\pm$  and  $\varrho$  are periodic in  $\phi$  with period  $\phi_0 = 2\pi$ . The period  $\phi_0$  has a deep physical meaning. In fact, recalling our convention  $c = \hbar = e = 1$ ,  $\phi_0$  equals precisely the elementary flux quantum  $2\pi\hbar c/e$  associated with a single charge  $e$  and appearing<sup>36</sup> in the context of Aharonov-Bohm type oscillations in non simply connected mesoscopic systems. Note also that

$$\varrho(k, \phi) = \varrho(k, -\phi), \quad \tau_-(k, \phi) = \tau_+(k, -\phi) \quad (15)$$

Hence, we can restrict  $\phi$  to  $[0, 2\pi]$  and even to  $[0, \pi]$  when dealing with quantities involving only  $\varrho$ . We emphasize that both  $\varrho$  and  $\tau_\pm$  are  $k$ -dependent, in spite of the fact that the local scattering matrices (4) are constant. This dependence is a direct consequence of the finite size of the ring. In fact, the momentum  $k$  enters  $\varrho$  and  $\tau_\pm$  only through the dimensionless combination  $kd$ . It follows from (8) that  $\varrho$  and  $\tau_\pm$  are  $2\pi/d$ -periodic in  $k$ , the shape of the oscillations being strongly influenced by the transmission  $\mathbf{t}$  and the flux  $\phi$ . The behavior of the probability  $\tau_-^2$  for  $d = 1$ , shown in fig. 3, confirms this statement. The dashed (black) and the continuous (red) lines describe the oscillations for  $\phi = 0$  (left) and  $\phi = \pi/4$  (right) for  $\mathbf{t} = 0.5$  and  $\mathbf{t} = 0.99$  respectively. As already observed, for  $\mathbf{t} \sim 1$  the external edges are almost isolated. Accordingly, in this regime, one expects very small transmission amplitudes. This is indeed the case with the exception of the momenta  $k = \frac{\pm\phi + 2\pi n}{3d}$ , characterized by the appearance of sharp peaks with maximum close to  $4/9$  and corrections of order  $1 - \mathbf{t}$ . For  $\phi \neq n\pi$ , there are six of them in each  $k$  interval of length  $2\pi/d$  and only three if  $\phi = n\pi$ . fig. 3 illustrates the phenomenon for  $\phi = 0$  (left) and  $\phi = \pi/4$  (right). Because of (14), the behavior of the reflection amplitude  $\varrho$  is complementary.

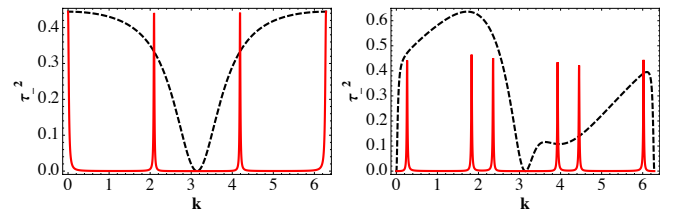


FIG. 3: (Color online)  $\tau_+^2(k, \phi, d = 1)$  for  $\mathbf{t} = 0.5$  (dashed black line) and  $\mathbf{t} = 0.99$  (continuous red line) for  $\phi = 0$  (left) and  $\phi = \pi/4$  (right).

We stress that at  $\mathbf{t} = 1$  the amplitudes  $\tau_\pm$  become actually *discontinuous* in  $k$ . One has indeed

$$\lim_{\mathbf{t} \rightarrow 1} \tau_\pm(k, \phi) = \begin{cases} \frac{2}{3}, & k = \frac{\pm\phi + 2\pi n}{3d}, \quad n \in \mathbb{Z}, \\ 0, & k \neq \frac{\pm\phi + 2\pi n}{3d}. \end{cases} \quad (16)$$

This special  $k$ -dependence of  $\tau_\pm$  for  $\mathbf{t} \sim 1$  is at the origin of the resonant tunneling effect on the current and the shot noise discussed below. Similar phenomena show up in the other limit  $\mathbf{t} \sim 0$ . In both cases, the external edges become almost disconnected, see (4). Thus, the resonant tunneling effect signals a kind of topology change.

Another type of discontinuities of  $\tau_\pm$ , which involves the magnetic flux and deserves attention, is described by

$$\lim_{k \rightarrow \frac{2l\pi}{d}} \tau_\pm(k, \phi) = \begin{cases} \frac{2}{3}, & \phi = n\phi_0, \quad l, n \in \mathbb{Z}, \\ 0, & \phi \neq n\phi_0. \end{cases} \quad (17)$$

This behavior is at the origin of the effect on the pure thermal noise at small temperatures discussed below.

#### IV. CURRENTS, CONDUCTANCE AND NOISE

To the end of the paper we study the non-equilibrium transport properties of the Y-junction in fig. 2 with thermal reservoirs at inverse temperatures  $\beta_i$  and chemical potentials

$$\mu_i = k_F - V_i, \quad i = 1, 2, 3, \quad (18)$$

where  $k_F$  defines the Fermi energy and  $V_i$  is the external voltage applied to the edge  $E_i$ . In what follows we keep  $k_F$  fixed, varying eventually the gate voltages  $V_i$ . The system is away from equilibrium if  $\mathbb{S}^\phi$  admits at least one non-trivial transmission coefficient among edges with different  $\beta_i$  and/or  $\mu_i$ . The corresponding non-equilibrium dynamics is implemented by a *steady state*  $\Omega_{\beta,\mu}$ , characterized by non-vanishing time-independent charge and heat currents circulating along the leads. The construction<sup>29</sup> of  $\Omega_{\beta,\mu}$  involves the scattering matrix  $\mathbb{S}^\phi$  and fully takes into account both the minimal coupling with the external magnetic field and the vertex interactions. We denote in what follows the expectation values in the state  $\Omega_{\beta,\mu}$  by  $\langle \dots \rangle_{\beta,\mu}$  and stress that the current correlation functions  $\langle j_x(t, x, i) \rangle_{\beta,\mu}$  and  $\langle j_x(t_1, x_1, i_1) j_x(t_2, x_2, i_2) \rangle_{\beta,\mu}$  used below are *exact*. No approximations, like linear response theory, are adopted.

For the one-point function one finds the Landauer-Büttiker<sup>30,31</sup> expression

$$J_i \equiv \langle j_x(t, x, i) \rangle_{\beta,\mu} = \int_0^\infty \frac{dk}{2\pi} \frac{k}{m} \sum_{j=1}^3 \left[ \delta_{ij} - |\mathbb{S}_{ij}^\phi(k)|^2 \right] d_j(k) \quad (19)$$

where

$$d_i(k) = \frac{e^{-\beta_i[\omega(k) - \mu_i]}}{1 + e^{-\beta_i[\omega(k) - \mu_i]}}, \quad \omega(k) = \frac{k^2}{2m}, \quad (20)$$

is the familiar Fermi distribution. The periodicity of  $|\sigma_i(k)|$  in  $\phi$  implies that  $J_i$  oscillate with period  $\phi_0$ . The unitarity of  $\mathbb{S}^\phi$  leads to the  $\mathbf{t}$ -independent bound

$$|J_i| \leq \frac{1}{2\pi\beta_i} \log \left[ 1 + e^{(k_F - V_i)\beta_i} \right], \quad (21)$$

on the amplitude of the oscillations. Introducing the variable  $\xi = k^2/2m$  and using that the Fermi distribution (20) approaches the Heaviside step function  $\theta(\mu_i - \xi)$  in the zero temperature limit  $\beta_i \rightarrow \infty$ , one obtains from (19)

$$J_i = \theta(\mu_i) \frac{\mu_i}{2\pi} - \sum_{j=1}^3 \theta(\mu_j) \int_0^{\mu_j} \frac{d\xi}{2\pi} \left| \mathbb{S}_{ij}^\phi \left( \sqrt{2m\xi} \right) \right|^2. \quad (22)$$

We will compare below (22) to the shot noise.

In order to get a more precise idea on the dependence of the current  $J_i$  on  $\phi$ , the transmission  $\mathbf{t}$  and the temperature  $\beta$ , we concentrate on (19). The  $k$ -integration can not be performed in a closed analytic form, but being well

defined, the integral can be computed numerically. The plots in fig. 4 illustrate the result for  $d = 1$ ,  $m = 1/2$ ,  $k_F = 3$ ,  $V_1 = -V_2 = -5$  and  $V_3 = 0$ . The first line displays  $J_1$  as a function of  $\mathbf{t}$  for  $\phi = 0$  (dashed line) and  $\phi = 2\pi/3$  (continuous line) at  $\beta_1 = \beta_2 = \beta_3 = 10$  (left) and  $\beta_1 = \beta_2 = \beta_3 = 0.1$  (right). As expected, the current vanishes at  $\mathbf{t} = 0, 1$ , when the external edges are isolated from each other. We see also that the position of the maximum of  $J_1$  depends on the flux and the temperature. In the second line of fig. 4 we report  $J_1$  as a function of  $\phi$  at  $\mathbf{t} = 0.4$  (dashed) and  $\mathbf{t} = 0.7$  (continuous), which show the expected oscillation in  $\phi$  with period  $\phi_0$ . The continuous (red) lines illustrate the impact of the higher harmonics  $n\phi_0$ , which become relevant for  $\mathbf{t} > 0.5$ .

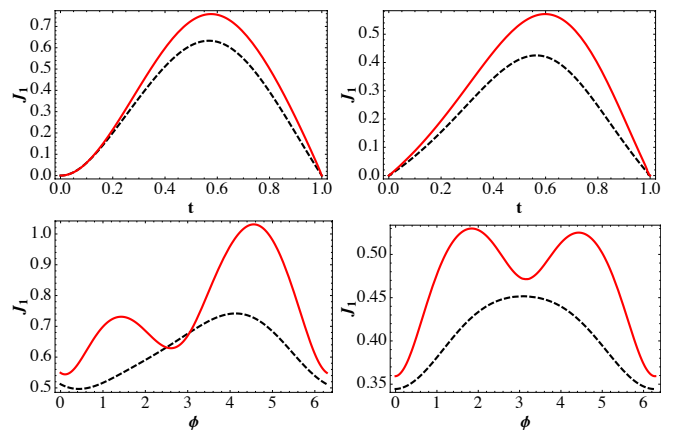


FIG. 4: (Color online)  $J_1(\phi, \mathbf{t})$  for fixed  $\phi$  (first line) and fixed  $\mathbf{t}$  (second line) at  $\beta_i = 10$  (left) and  $\beta_i = 0.1$  (right).

The *zero frequency noise power* is defined as usual<sup>32</sup> by

$$P_{ij} = \lim_{\nu \rightarrow 0^+} \int_{-\infty}^{\infty} dt e^{i\nu t} \langle j_x(t, x_1, i) j_x(0, x_2, j) \rangle_{\beta,\mu}^{\text{conn}}, \quad (23)$$

where  $\langle j_x(t_1, x_1, i) j_x(t_2, x_2, j) \rangle_{\beta,\mu}^{\text{conn}}$  is the *connected* current-current correlation function in the state  $\Omega_{\beta,\mu}$ . It turns out<sup>29</sup> that  $P_{ij}$  is  $x_{1,2}$ -independent and is given by

$$P_{ij} = \frac{1}{m} \int_0^\infty \frac{dk}{2\pi} k \left\{ \delta_{ij} D_{ii}(k) - |\mathbb{S}_{ij}^\phi(k)|^2 D_{jj}(k) - |\mathbb{S}_{ji}^\phi(k)|^2 D_{ii}(k) + \sum_{l,m=1}^3 \mathcal{F}_{ijlm}(k) [D_{lm}(k) + D_{ml}(k)] \right\} \quad (24)$$

where

$$\mathcal{F}_{ijlm}(k) = \frac{1}{2} \mathbb{S}_{il}^\phi(k) \overline{\mathbb{S}}_{jl}^\phi(k) \mathbb{S}_{jm}^\phi(k) \overline{\mathbb{S}}_{im}^\phi(k) \quad (25)$$

and  $D_{ij}(k) \equiv d_i(k)[1 - d_j(k)]$ .  $P_{ij}$  is a symmetric matrix. To study the thermal noise, we assume  $\mu_i = \mu$  and  $\beta_i = \beta$ . Using the Kirchhoff rule  $\sum_{i=1}^3 P_{ij} = 0$ , we get the circulant matrix

$$P_{ij} = P(3\delta_{ij} - 1)/2 \quad (26)$$

where

$$P \equiv P(T, \phi) = \frac{2}{m} \int_0^\infty \frac{dk}{2\pi} k D(k) [\tau_-^2(k, \phi) + \tau_+^2(k, \phi)] \quad (27)$$

with  $D(k) \equiv d(k)[1 - d(k)]$  and  $T = 1/\beta$ . Like the conductance,  $P$  oscillates in  $\phi$  with period  $\phi_0$ . From (15),  $P$  is an even function of  $\phi$  so it is enough to study it on  $[0, \pi]$ . The bound on the amplitude, following from unitarity is now

$$0 \leq P \leq \frac{2}{m} \int_0^\infty \frac{dk}{2\pi} k D(k) = \frac{1}{\pi\beta(1 + e^{-\beta\mu})}. \quad (28)$$

Define

$$g(T, \phi) = \frac{\partial \ln P(T, \phi)}{\partial \ln T}. \quad (29)$$

The numerical study confirms that  $g = 1$  at large temperatures  $T \rightarrow \infty$ , independently of the flux  $\phi$ . In this regime one recovers therefore the well-known Johnson-Nyquist behavior  $P \sim T$ . The situation changes drastically as  $T \rightarrow 0$ . For  $\mu = 0$ , the pure thermal noise has the following power law type behavior as  $T \rightarrow 0$

$$g(T, \phi) = \begin{cases} 1, & \phi = 0, \\ \eta(\phi), & 0 \leq \phi \leq \phi_c, \\ 2, & \phi_c \leq \phi \leq \pi, \end{cases} \quad (30)$$

where the critical value  $\phi_c$  scales like  $(mT)^{\frac{1}{4}}$ . We have numerical evidence that  $\eta$ , as a function of  $\phi/\phi_c$ , is a universal  $T$ -independent profile, interpolating between the linear ( $g = 1$  at  $\phi = 0$ ) and quadratic ( $g = 2$  for  $\phi > \phi_c$ ) behavior of  $P$ . This was checked over four orders of magnitude in temperature and is shown in fig. 5.

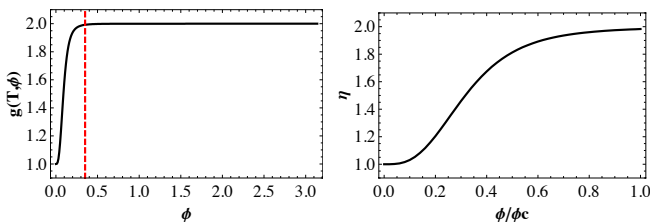


FIG. 5: (Color online) Left: full behavior of  $g(T, \phi)$  (for  $T = 10^{-5}$  and other parameters as before). Dashed line shows  $\phi_c$ . Right: universal profile  $\eta$  as a function of the rescaled flux  $\phi/\phi_c$  (zoom of the interpolation region).

Therefore, we conclude that a nonzero magnetic flux in the Y-junction implies a significant modification of the Johnson-Nyquist law at small temperature. This new feature provides an interesting signature of a physical effect that hopefully can be observed experimentally.

Let us investigate finally the shot noise following from eq.(24). For this purpose we set  $\beta_i = \beta$  and take the

$\beta \rightarrow \infty$  limit, keeping  $\mu_i > 0$  arbitrary. Adopting the variable  $\xi = k^2/2m$  one gets

$$P_{ij} = \sum_{l \neq m=1}^3 \varepsilon(\mu_l - \mu_m) \int_{\mu_m}^{\mu_l} \frac{d\xi}{2\pi} \mathcal{F}_{ijlm}(\sqrt{2m\xi}), \quad (31)$$

$\varepsilon$  being the sign function. Note that since  $P_{ij}$  is symmetric and satisfies the Kirchhoff rule, we only need to compute the diagonal elements  $P_{ii}$  in order to reconstruct the complete matrix. Indeed, one has  $P_{ij} = \frac{1}{2}(P_{kk} - P_{ii} - P_{jj})$  for mutually distinct  $i, j, k$  and the diagonal elements read

$$P_{ii} = 2 \sum_{l < m=1}^3 \varepsilon(\mu_l - \mu_m) \int_{\mu_m}^{\mu_l} \frac{d\xi}{2\pi} \mathcal{F}_{iilm}(\sqrt{2m\xi}). \quad (32)$$

Assuming for definiteness that  $\mu_1 < \mu_2 < \mu_3$ , one obtains

$$P_{11} = \int_{\mu_1}^{\mu_2} \frac{d\xi}{2\pi} \varrho^2(1 - \varrho^2) + \int_{\mu_2}^{\mu_3} \frac{d\xi}{2\pi} \tau_-^2(1 - \tau_-^2), \quad (33)$$

$$P_{22} = \int_{\mu_1}^{\mu_2} \frac{d\xi}{2\pi} \tau_-^2(1 - \tau_-^2) + \int_{\mu_2}^{\mu_3} \frac{d\xi}{2\pi} \tau_+^2(1 - \tau_+^2), \quad (34)$$

$$P_{33} = \int_{\mu_1}^{\mu_2} \frac{d\xi}{2\pi} \tau_+^2(1 - \tau_+^2) + \int_{\mu_2}^{\mu_3} \frac{d\xi}{2\pi} \varrho^2(1 - \varrho^2), \quad (35)$$

where  $\varrho$  and  $\tau_{\pm}$  are computed at  $k = \sqrt{2m\xi}$ . Compared to the pure thermal noise (26,27), the shot noise involves the fourth order powers of  $\varrho$  and  $\tau_{\pm}$  as well. Their dependence on  $\phi$  implies that  $P_{ii}$  oscillate with period  $\phi_0$ . The amplitude is subject to the obvious unitarity bound

$$0 \leq P_{ii} \leq \mu_3 - \mu_1. \quad (36)$$

We study finally the behavior of the shot noise as a function of the chemical potentials  $\mu_i$ , or equivalently, the voltages  $V_i$  in (18). It is instructive to do this, comparing  $P_{ii}$  with the zero-temperature steady current  $J_i$  given by (22), and the transmission amplitude  $\tau_{\pm}$ . For this purpose we fix  $m = 1/2$ ,  $\mu_1 = \mu_2 = d = 1$  and vary  $\mu_3$ . In this regime

$$J_1(\phi) = - \int_1^{\mu_3} \frac{d\xi}{2\pi} \tau_-^2, \quad P_{11}(\phi) = \int_1^{\mu_3} \frac{d\xi}{2\pi} \tau_-^2(1 - \tau_-^2). \quad (37)$$

An interesting resonant tunneling effect, depending on  $\phi$ , is observed for  $\mathbf{t} \sim 1$ . This corresponds to the situation where the external edges are weakly coupled to the ring. The peaks in the transmission amplitudes  $\tau_{\pm}$ , shown in fig. 3, can be interpreted as resonances corresponding to eigenstates of the ring. A similar situation was discussed in<sup>3,34</sup> in the case of the ring with two external edges and the same physical interpretation holds here. As the voltage is increased, these resonances generate plateaux in the shot noise  $P_{ii}$  and the current  $J_i$ . This fact is illustrated in fig. 6, where we plotted  $\tau_-^2(\sqrt{\mu_3})/2\pi$  (continuous red curve),  $P_{11}(\mu_3)$  (dashed black curve) and  $J_1(\mu_3)$  (dotted blue curve). Switching on the magnetic field changes the location of the peaks and hence the location of the jumps from one plateau to the next.

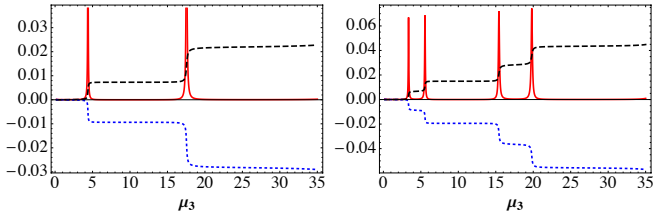


FIG. 6: (Color online) Plots of  $P_{11}$  (black dashed),  $J_1$  (blue dotted) and  $\tau^2/2\pi$  (red continuous) at  $t = 0.99$  for  $\phi = 0$  (left) and  $\phi = \pi/4$  (right).

## V. CONCLUSIONS

The transport properties of fermions in a Y-junction with a finite size ring, connected to thermal reservoirs and crossed by magnetic flux  $\phi$ , have been investigated. The bulk dynamics is described by the Schrödinger equation with the minimal coupling to an ambient electromagnetic field. At the vertices, the most general scale invariant local interactions, compatible with a unitary time evolution, are considered. The exact expression for the total scattering matrix  $S^\phi$  of the system is fundamental for our investigation. The non-equilibrium dynamics, generated by the contact to the heat baths, is

captured by steady states  $\Omega_{\beta,\mu}$  incorporating  $S^\phi$ . It is essential that our framework does not rely on conformal symmetry, thus allowing us to investigate directly a finite size ring. The conductance and the noise power are extracted from the current correlation functions in the state  $\Omega_{\beta,\mu}$ . We find a resonant tunneling effect when the ring is weakly coupled to the external leads. Another interesting phenomenon concerns the influence of the magnetic flux on the noise (and conductance). For  $\phi \neq 0$ , we found a drastic departure from the linear Johnson-Nyquist law for small temperatures. Let us mention in this respect that the same analysis applies to a Dirac Y-junction which shows an interpolation between linear and *cubic* (instead of quadratic) power law behavior, the difference being a consequence of the linear dispersion relation of the Dirac equation<sup>35</sup>. To investigate dephasing effects<sup>37</sup> in the transport along the ring, one should introduce electron-electron bulk interaction in the framework.

All the physical information about the Y-junction has been extracted in our discussion from the one-point and two-point current correlation functions. It will be interesting to extend the above analysis to the higher correlators, thus investigating the effect of the magnetic flux on the full counting statistics<sup>38</sup>, which provides further details about the system.

- 
- <sup>1</sup> C. Nayak, M. P. A. Fisher, A. W. W. Ludwig and H. H. Lin, Phys. Rev. B **59** (1999) 15694.  
<sup>2</sup> I. Safi, P. Devillard, and T. Martin, Phys. Rev. Lett. **86** (2001) 4628.  
<sup>3</sup> S. Rao and D. Sen, Phys. Rev. B **70** (2004) 195115.  
<sup>4</sup> B. Bellazzini, M. Mintchev and P. Sorba, J. Phys. A **40** (2007) 2485.  
<sup>5</sup> C.-Y. Hou and C. Chamon, Phys. Rev. B **77** (2008) 155422.  
<sup>6</sup> S. Das and S. Rao, Phys. Rev. B **78** (2008) 205421.  
<sup>7</sup> B. Bellazzini, P. Calabrese and M. Mintchev, Phys. Rev. B **79** (2009) 085122.  
<sup>8</sup> B. Bellazzini, M. Mintchev and P. Sorba, Phys. Rev. B **80** (2009) 25441.  
<sup>9</sup> B. Bellazzini, M. Mintchev and P. Sorba, Phys. Rev. B **82** (2010) 195113.  
<sup>10</sup> S. Lal, S. Rao, and D. Sen, Phys. Rev. B **66** (2002) 165327.  
<sup>11</sup> X. Barnabe-Theriat, A. Sedeki, V. Meden, K. Schönhammer, Phys. Rev. Lett. **94** (2005) 136405.  
<sup>12</sup> S. Das, S. Rao, D. Sen, Phys. Rev. B **74** (2006) 045322.  
<sup>13</sup> S. Das, S. Rao and A. Saha, Phys. Rev. B **79** (2009) 155416.  
<sup>14</sup> A. Soori and D. Sen, Europhys. Lett. **93** (2011) 57007.  
<sup>15</sup> D. N. Aristov, Phys. Rev. B **83** (2011) 115446.  
<sup>16</sup> D. N. Aristov and P. Wölfle, Phys. Rev. B **84** (2011) 155426.  
<sup>17</sup> M. Oshikawa, C. Chamon, and I. Affleck, J. Stat. Mech. (2006) P02008.  
<sup>18</sup> A. Rahmani, C.-Y. Hou, A. Feiguin, M. Oshikawa, C. Chamon and I. Affleck, Phys. Rev. B **85** (2012) 045120.  
<sup>19</sup> V. Kstrykin and R. Schrader, J. Phys. A: Math. Gen. **32** (1999) 595; Fortschr. Phys. **48** (2000) 703.  
<sup>20</sup> V. Kstrykin and R. Schrader, Commun. Math. Phys. **237** (2003) 161.  
<sup>21</sup> M. Harmer, J. Phys. A **33** (2000) 9015.  
<sup>22</sup> B. Bellazzini and M. Mintchev, J. Phys. A **39** (2006) 11101.  
<sup>23</sup> B. Bellazzini, M. Burrello, M. Mintchev and P. Sorba, Proc. Symp. Pure Math. **77** (2008) 639.  
<sup>24</sup> V. Kstrykin, R. Schrader, J. Math. Phys. **42** (2001) 1563.  
<sup>25</sup> M. Mintchev and E. Ragoucy, J. Phys. A **40** (2007) 9515.  
<sup>26</sup> E. Ragoucy, J. Phys. A **42** (2009) 295205.  
<sup>27</sup> S. Khachatryan, A. Sedrakyan and P. Sorba, Nucl. Phys. B **825** (2010) 444.  
<sup>28</sup> V. Caudrelier, E. Ragoucy, Nucl. Phys. B **828** (2010) 515.  
<sup>29</sup> M. Mintchev, J. Phys. A **44** (2011) 415201.  
<sup>30</sup> R. Landauer, IBM J. Res. Dev. **1** (1957) 233; Philos. Mag. **21** (1970) 863.  
<sup>31</sup> M. Büttiker, Phys. Rev. Lett. **57** (1986) 1761; IBM J. Res. Dev. **32** (1988) 317.  
<sup>32</sup> Ya. Blanter and M. Büttiker, Phys. Rep. **336** (2000) 1.  
<sup>33</sup> Y. Gefen, Y. Imry and M. Ya. Azbel, Phys. Rev. Lett. **52** (1984) 129.  
<sup>34</sup> M. Büttiker, Y. Imry and M. Ya. Azbel, Phys. Rev. A **30** (1984) 1982.  
<sup>35</sup> V. Caudrelier, M. Mintchev, E. Ragoucy, in preparation.  
<sup>36</sup> A. G. Aronov and Yu. V. Sharvin, Rev. Mod. Phys. **59** (1987) 755.  
<sup>37</sup> A. P. Dmitriev, I. V. Gornyi, V. Yu. Kachorovskii, and D. G. Polyakov, Phys. Rev. Lett. **105** (2010) 036402.  
<sup>38</sup> L. S. Levitov, H.-W. Lee and G. B. Lesovik, J. Math. Phys. **37** (1996) 4845.